THE JOURNAL OF PHYSICAL CHEMISTRY B

ARTICLE

pubs.acs.org/JPCB

Exploring the Effect of Side-Chain Substitutions upon the Secondary Structure Preferences of β-Peptides

Zhixiong Lin and Wilfred F. van Gunsteren*

Laboratory of Physical Chemistry, Swiss Federal Institute of Technology, ETH, 8093 Zürich, Switzerland

ABSTRACT: The ability to design well-folding β-peptides with a specific biological activity requires detailed insight into the relationship between the β-amino acid sequence and the dominant three-dimensional structure of such a peptide. To this end, secondary structure preferences of two sets of 16 β-peptides were investigated by means of one-step perturbation using molecular dynamics (MD) simulations. For each set of peptides, two reference-state simulations and one perturbed-state simulation were carried out to predict the secondary structure preferences for the other 15 peptides. The results show that the substitution of a methyl group in the third or fourth residue stabilizes the left-handed 3_{14}-helix over the right-handed $2.7_{10/12}$-helix for the set of hexapeptides **A**; for the set of heptapeptides **B**, having methyl substitutions at both β- and α-carbon positions of the fourth or fifth residue stabilizes the left-handed 3_{14}-helix over the right-handed 2.5_{12}-helix. Not only the side-chain substitution pattern but also the side-chain composition affects the relative stability of different secondary structures. The approach described here may be of use in peptide design with an eye to obtaining peptides with particular folds and biological activities.

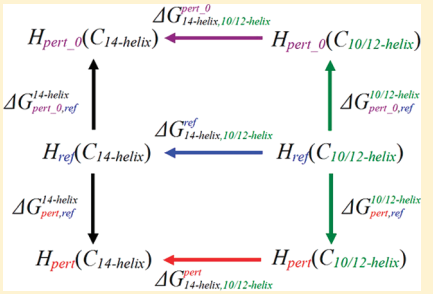

1. INTRODUCTION

Understanding the folding process of proteins or polypeptides is one of the major challenges in molecular biology.[1,2] Our understanding of the folding process has advanced considerably during the past decade because of the improvement of experimental techniques and the development of computational methods.[3,4] Now, molecular dynamics (MD) simulation of the folding equilibria of polypeptides has become feasible,[5−7] while it is still not yet possible to simulate the folding equilibria of larger proteins.

β-peptides[8] are ideal systems to investigate the folding process because they can fold into stable secondary structures for relatively short chain lengths when solvated in methanol. Having two sp^3 carbon atoms in the backbone of each residue, their folded conformation is not only influenced by the side-chain sequence but also by the substitution pattern.[9] Previous experiments,[10] quantum-chemical calculations,[11−13] and MD simulations[14,15] have shown that β-peptides with substitution exclusively at the β-carbon atom (β^3-peptides) preferentially adopt a left-handed 3_{14}-helical conformation, while an alternating substitution pattern at the α- and β-carbon atoms (β^2/β^3-peptides) induces a right-handed $2.7_{10/12}$-helix. It would be of interest to further investigate the effect of side-chain substitution patterns on the secondary structure preferences of β-peptides. However, a systematic study is computationally too expensive because of the exponentially growing number of possible side-chain combinations along the peptide chain. In addition, for peptides with a strong preference toward a certain fold, it would be difficult to obtain an estimation of the free energy difference between other secondary structures and this fold due to the lack of sampling of the former unstable conformations.

The one-step perturbation method allows one to obtain many free energy differences from only one or few MD simulations.[16] It has been successfully applied to calculate solvation free energies,[17] relative binding free energies,[18] and folding free energies as a function of force-field parameters.[19,20] Recently, one-step perturbation was applied to calculate free energies of folding for peptides with different side-chain substitutions.[21−23] The results are consistent with both experimental data and long-time MD simulation results. These studies regarded only peptides that preferred one dominant helical conformational, a 3_{14}-helical fold.

Here, we go one step further and investigate two β-peptides (Figure 1) that may each adopt two different, right-handed and left-handed, helical folds.[10,24,25] We use one-step perturbation and only three MD simulations per peptide to study the effect of 16 side-chain substitution patterns on the secondary structure preferences of these two sets of β-peptides. This is a challenge because sampling of transitions between different left- and right-handed helical structures in a single simulation is difficult.

2. METHODS

2.1. One-Step Perturbation. The principle of one-step perturbation is described in refs 19 and 21−23. Here we only present the essential equations, and we refer to ref 22 for the details. The free enthalpy difference between two secondary structures for peptide **A**, i.e., $\Delta G_{14\text{-helix},10/12\text{-helix}}$, can be calculated

Received: June 7, 2011
Revised: September 19, 2011
Published: October 03, 2011

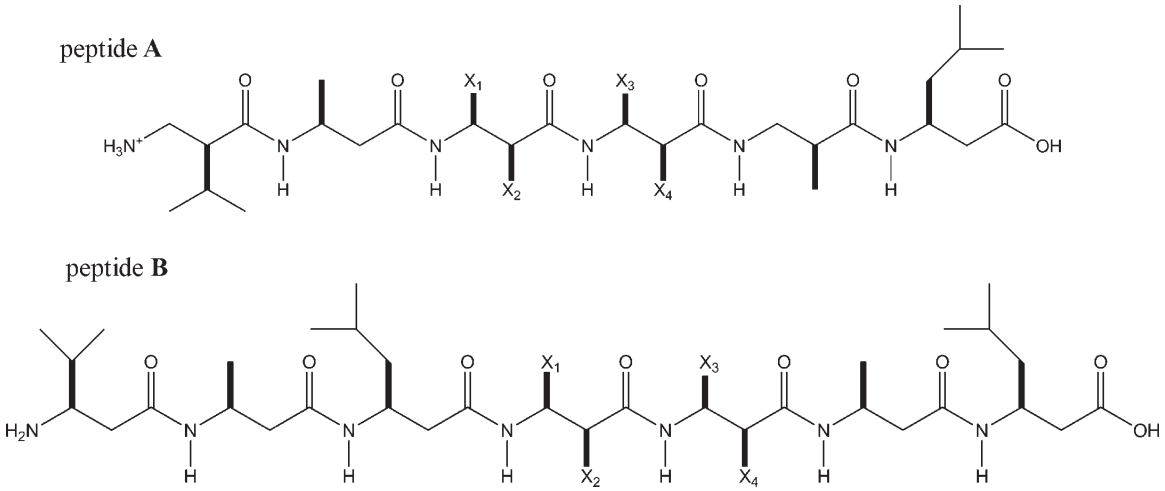

Figure 1. Chemical formulas of the two β-peptides studied.[10,24] Peptide **A**: H_2^+-β^2-HVal-β^3-HAla-(S,S)-β^3-$HX_1(\alpha X_2)$-(S,S)-β^3-$HX_3(\alpha X_4)$-β^2-HAla-β^3-HLeu-OH. Reproduced with permission from ref 10. Copyright 1998 Verlag Helvetica Chimica Acta. Peptide **B**: H-β^3-HVal-β^3-HAla-β^3-HLeu-(S,S)-β^3-$HX_1(\alpha X_2)$-(S,S)-β^3-$HX_3(\alpha X_4)$-β^3-HAla-β^3-HLeu-OH, where X_1 to X_4 denote soft-core atoms in the reference states and CH_3 or H in the perturbed-state real peptides. Reproduced with permission from ref 24. Copyright 1996 Verlag Helvetica Chimica Acta.

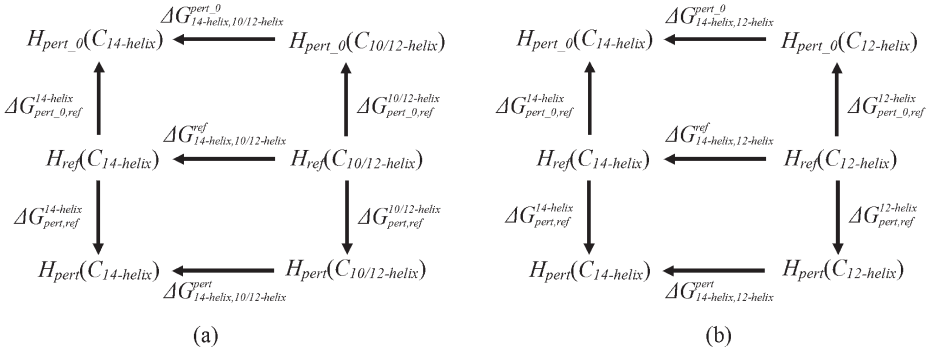

Figure 2. Schematic representation of thermodynamic cycles used for peptide **A** (a) and peptide **B** (b). H_{ref} and H_{pert} refer to reference and perturbed Hamiltonians, respectively, and the conformational ensembles belonging to these Hamiltonians are separated into subensembles of different secondary structures. The upper parts of the cycles are constructed through an additional Hamiltonian H_{pert_0}, with which the free enthalpy between two secondary structures can be calculated from a single MD simulation using eq 1.

from a single simulation using

$$\Delta G_{14\text{-helix},\,10/12\text{-helix}} = -k_B T \ln(N_{14\text{-helix}}/N_{10/12\text{-helix}}) \quad (1)$$

where $N_{14\text{-helix}}$ or $N_{10/12\text{-helix}}$ denotes the number of configurations belonging to the secondary structure $C_{14\text{-helix}}$ or $C_{10/12\text{-helix}}$, respectively, and k_B is the Boltzmann constant and T the temperature.

According to statistical mechanics,[26] the free enthalpy change of a conformational state C due to changing the Hamiltonian from H_{ref} to H_{pert} is given by

$$\Delta G^{C}_{pert,\,ref} = -k_B T \ln\langle e^{-(H_{pert} - H_{ref})/k_B T}\rangle_{ref,\,C} \quad (2)$$

where the ensemble averaging denoted by $\langle ...\rangle$ is carried out over all configurations that were generated using H_{ref} and that belong to the conformational state C. According to the thermodynamic cycle shown in the lower part of Figure 2a, we have

$$\Delta G^{pert}_{14\text{-helix},\,10/12\text{-helix}} = \Delta G^{ref}_{14\text{-helix},\,10/12\text{-helix}} + \Delta G^{14\text{-helix}}_{pert,\,ref} - \Delta G^{10/12\text{-helix}}_{pert,\,ref} \quad (3)$$

Thus, we may derive the free enthalpy differences $\Delta G^{pert}_{14\text{-helix},10/12\text{-helix}}$ for many different perturbed-state Hamiltonians H_{pert} from a single simulation using a possibly unphysical reference-state Hamiltonian H_{ref}.

However, in some cases it is very difficult to obtain accurate $\Delta G^{ref}_{14\text{-helix},10/12\text{-helix}}$ values from a single simulation using eq 1. Then only the relative free enthalpies can be obtained, i.e., $\Delta G^{pert}_{14\text{-helix},10/12\text{-helix}} - \Delta G^{ref}_{14\text{-helix},10/12\text{-helix}}$. This situation may be resolved by constructing an additional thermodynamic cycle shown in the upper part of Figure 2a, which contains a simulation of one perturbed-state Hamiltonian H_{pert_0}. If in this simulation both conformational states are sampled simultaneously, it yields an accurate $\Delta G^{pert\_0}_{14\text{-helix},10/12\text{-helix}}$ value. Combining the upper and lower thermodynamic cycles in Figure 2a, one has

$$\Delta G^{pert}_{14\text{-helix},\,10/12\text{-helix}} = \Delta G^{pert\_0}_{14\text{-helix},\,10/12\text{-helix}} - \Delta G^{14\text{-helix}}_{pert\_0,\,ref} + \Delta G^{10/12\text{-helix}}_{pert\_0,\,ref} + \Delta G^{14\text{-helix}}_{pert,\,ref} - \Delta G^{10/12\text{-helix}}_{pert,\,ref} \quad (4)$$

Thus, from three simulations, i.e., one using a reference-state Hamiltonian H_{ref} that samples the 3_{14}-helical conformation, one

Table 1. Overview of the Reference- and Perturbed-State Simulations

peptide	simulation name	ref/pert.[a]	H-bond restraints	soft-core interactions	substitution at given X: X_1	X_2	X_3	X_4	no. of solvent molecules	simulation time (ns)
peptide **A**	RA_{14}	ref	3_{14}-helix	yes	CH_3	CH_3	CH_3	CH_3	1131	110
	$RA_{10/12}$	ref	$2.7_{10/12}$-helix	yes	CH_3	CH_3	CH_3	CH_3	1131	110
	P_A	pert.	no	no	H	CH_3	CH_3	H	1124	500
peptide **B**	RB_{14}	ref	3_{14}-helix	yes	CH_3	CH_3	CH_3	CH_3	1095	110
	RB_{12}	ref	2.5_{12}-helix	yes	CH_3	CH_3	CH_3	CH_3	1095	110
	P_B	pert.	no	no	CH_3	CH_3	CH_3	H	1096	500

[a] Ref: reference-state simulation; pert.: perturbed-state simulation.

using a reference-state Hamiltonian H_{ref} that samples the $2.7_{10/12}$-helical conformation, and one using a perturbed-state Hamiltonian H_{pert_0} that samples both conformations, we can obtain the free enthalpy differences between the $C_{14\text{-helix}}$ and $C_{10/12\text{-helix}}$ conformations for the remaining 15 perturbed-state Hamiltonians. Similarly, the thermodynamic cycles for peptide **B** are shown in Figure 2b.

2.2. Molecular Model. Peptide **A** was modified from peptide **2** in ref 25. The side chains of the third and fourth residues were changed (Figure 1) in order to study the effect of different substitution patterns of these residues on the secondary structure preference of the peptide. The original peptide with substitution pattern X_1 = H, X_2 = $CH_2CH(CH_3)_2$, X_3 = $CH(CH_3)_2$, and X_4 = H folds into a right-handed $2.7_{10/12}$-helix and a left-handed 3_{14}-helix.[14,25] Peptide **B** was modified from peptide **1** in ref 25. The side chains of the fourth and fifth residues were changed. The original peptide with substitution pattern X_1 = CH_3, X_2 = CH_3, X_3 = $CH(CH_3)_2$, and X_4 = H folds into a left-handed 3_{14}-helix and a right-handed 2.5_{12}-helix.[25,27]

The simulations of the two β-peptides (Figure 1) were carried out in explicit solvent methanol using the GROMOS05 simulation package[28,29] and the GROMOS force-field parameter set 45A3.[30] The methanol solvent molecules were represented using a rigid three-site model belonging to the standard GROMOS set of solvents. Aliphatic CH_n groups were treated as united atoms, both in the solute and solvent. The N- and C-termini of peptide **A** and the C-terminus of peptide **B** were protonated. The unusual choice of the N-terminus of peptide **B**, i.e., NH_2 instead of NH_3^+, is because, among different protonation states, only the peptide with this one, i.e., NH_2 and COOH, folded into two different helical folds.[25] No counterion was used.

2.3. Simulation Setup. Two types of simulations were performed (Table 1). For each peptide, in the two reference simulations, the atoms X_{1-4} in Figure 1 are modeled as the so-called soft-core atoms, which allow the use of the perturbation formula eq 2 to obtain accurate free enthalpy differences between the perturbed states and the reference states. In the perturbed-state simulation, the free enthalpy between two helical conformations of a real peptide is obtained using eq 1.

The folded structures of the $2.7_{10/12}$-helix and the 3_{14}-helix served as the initial structure for the simulations of peptide **A** and peptide **B**, respectively. Periodic boundary conditions were applied on the basis of a rectangular box. A minimum distance of 1.4 nm between any peptide atom and the closest box wall was enforced while solvating the peptide. The resulting numbers of solvent molecules are listed in Table 1. After a steepest descent energy minimization to remove close contacts between solute and solvent atoms, an equilibration scheme was carried out which included sampling the atom velocities from a Maxwell distribution at 60 K and gradually raising the simulation temperature to 340 K, while decreasing the strength of the position-restraining potential energy term for the solute atoms.

Table 2. Restrained Hydrogen-Bonding O−H Pairs Used in Different Reference-State Simulations of the Two Peptides

peptide	conformation	H-bond restraint O−H pair
peptide **A**	3_{14}-helix	NH(2)···O(4)
		NH(3)···O(5)
		NH(4)···O(6)
	$2.7_{10/12}$-helix	NH(3)···O(4)
		NH(4)···O(1)
		NH(6)···O(3)
peptide **B**	3_{14}-helix	NH(2)···O(4)
		NH(3)···O(5)
		NH(4)···O(6)
		NH(5)···O(7)
	2.5_{12}-helix	NH(4)···O(1)
		NH(5)···O(2)
		NH(6)···O(3)
		NH(7)···O(4)

The simulations were carried out at constant temperature, 340 K, and constant pressure, 1 atm. This temperature is higher than physiological temperature and was chosen to enhance the sampling of the folding equilibrium. Simulation at room temperature would have shifted the conformational distribution strongly toward the folded conformation.[31,32] The simulation time is shown in Table 1. The solute molecules and the methanol solvent were separately coupled to a temperature bath by means of weak coupling,[33] using a coupling time of 0.1 ps. The pressure was calculated with an atomic virial and held constant by weak coupling[33] to an external pressure bath with a coupling time of 0.5 ps, using an isothermal compressibility of 4.575×10^{-4} (kJ mol^{-1} nm^{-3})$^{-1}$. All bond lengths and the geometry of the methanol molecules were constrained using the SHAKE algorithm[34] with a relative geometric accuracy of 10^{-4}, allowing a time step of 2 fs in the leapfrog algorithm to integrate the equations of motion. For the treatment of the nonbonded interactions twin-range cutoff radii of 0.8/1.4 nm were used. Interactions within 0.8 nm were evaluated every time step, the intermediate range interactions were updated every fifth time step, and the long-range electrostatic interactions beyond 1.4 nm

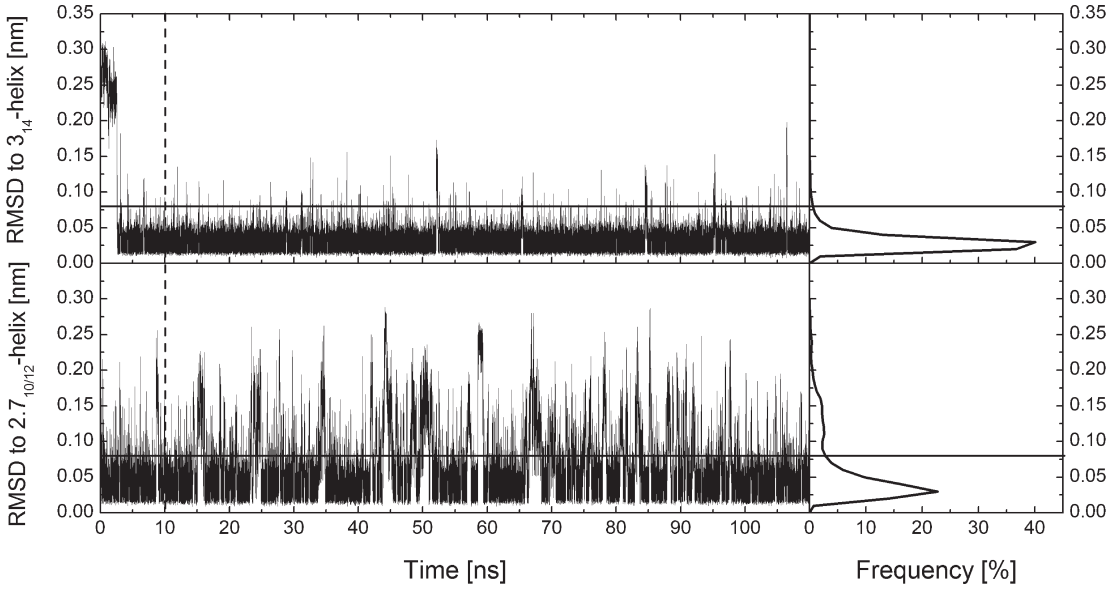

Figure 3. Time evolutions and distributions of the backbone atom-positional rmsd of residues 2−5 of the reference simulations of peptide **A**. Upper panels: Simulation RA_{14} with respect to the 3_{14}-helix. Lower panels: Simulation $RA_{10/12}$ with respect to the $2.7_{10/12}$-helix. The gray lines represent the criterion, an rmsd of 0.08 nm, used to distinguish folded and unfolded conformations. The first 10 ns were used as equilibration and excluded from calculating distributions.

were approximated by a reaction field force[35] according to a dielectric continuum with a dielectric permittivity of 17.7, the value of the dielectric permittivity of the methanol model.[36]

In the reference-state simulations, intrasolute hydrogen-bond restraints were applied. The restrained hydrogen bonds for the two conformational states of both peptides are listed in Table 2. For the pair of O and H atoms of each restrained hydrogen bond, the restraining potential energy term has a half-harmonic form, exerting an attractive force when the atomic O−H distance is above 0.25 nm. The restraining force constant was 100.0 kJ mol^{-1} nm^{-2}. We used soft-core Lennard-Jones interactions[37] instead of the normal Lennard-Jones ones for the interactions between atoms X_i and other atoms (Figure 1),

$$V(r_{ij}) = \frac{C_{12}^{ij}}{\left[\alpha_{LJ}\lambda^2(C_{12}^{ij}/C_6^{ij}) + r_{ij}^6\right]^2} - \frac{C_6^{ij}}{\left[\alpha_{LJ}\lambda^2(C_{12}^{ij}/C_6^{ij}) + r_{ij}^6\right]} \quad (5)$$

where r_{ij} is the distance between atoms i and j, C_{12}^{ij} and C_6^{ij} are the Lennard-Jones parameters for atom pair (i, j), $\lambda = 0.5$, and $\alpha_{LJ} = 1.51$ is a positive constant controlling the softness of the soft-core atoms.[21,37] The Lennard-Jones parameters of atom type CH_3 were used for atoms X_{1-4}.

2.4. Analysis. Trajectory coordinates and energies were stored every 0.5 ps. Atom-positional root-mean-square deviations (rmsd) were calculated after translational superposition of solute centers of mass and rotational least-squares fitting of the atomic coordinates of all backbone atoms (N, CB, CA, C) except for those in the N- and C-terminal residues of the β-peptides. An rmsd of 0.08 nm for peptide **A** and 0.10 nm for peptide **B** with respect to the ideal helical structures were used as the criteria to define secondary structures.[14,38]

For the perturbation free enthalpy calculations, the first 10 ns trajectories were used as the equilibration period, and the final 100 ns was used to calculate the perturbation free enthalpies. We did perturbations from the reference-state to the perturbed-state peptides with X_{1-4} as H or CH_3 (Figure 1); i.e., for $2^4 = 16$ real peptides. The H atom was modeled as a dummy atom without electrostatic or Lennard-Jones interactions while keeping the bonded interactions as for a CH_3 united atom, and CH_3 was modeled as a united atom as in the GROMOS force field, keeping its bonded interactions.

Because hydrogen-bond restraints were used when generating the reference-state ensembles, the restraining potential-energy terms should be considered as well in the perturbation free enthalpy calculations,

$$\Delta G^{C}_{pert,ref} = -k_B T \ln\langle e^{-[H_{phys\_pert} - (H_{phys\_ref} + H_{restr})]/k_B T}\rangle_{ref,C} \quad (6)$$

in which H_{phys} and H_{restr} denote the physical and the restraining parts of the Hamiltonian, respectively.

3. RESULTS AND DISCUSSION

3.1. Peptide A. For peptide **A**, the backbone atom-positional rmsds with respect to the left-handed 3_{14}-helix or the right-handed $2.7_{10/12}$-helix, respectively, of the two reference-state simulations are shown in Figure 3. An rmsd of 0.08 nm (gray horizontal line) was chosen as the criterion to define the different helical conformations $C_{14\text{-helix}}$ and $C_{10/12\text{-helix}}$. The peptide mainly sampled the folded conformations because of the hydrogen-bond restraining. Due to a low restraining force constant, unfolding events also occurred during both reference simulations.

The backbone atom-positional rmsds of the simulation P_A of H_{pert_0} with respect to the left-handed 3_{14}-helix and the right-handed $2.7_{10/12}$-helix are shown in Figure 4. Many transitions between the two helical conformations were sampled during the 500 ns simulation, promising an accurate value for $\Delta G^{pert\_0}_{14\text{-helix},10/12\text{-helix}}$. The fractions of the folded conformation

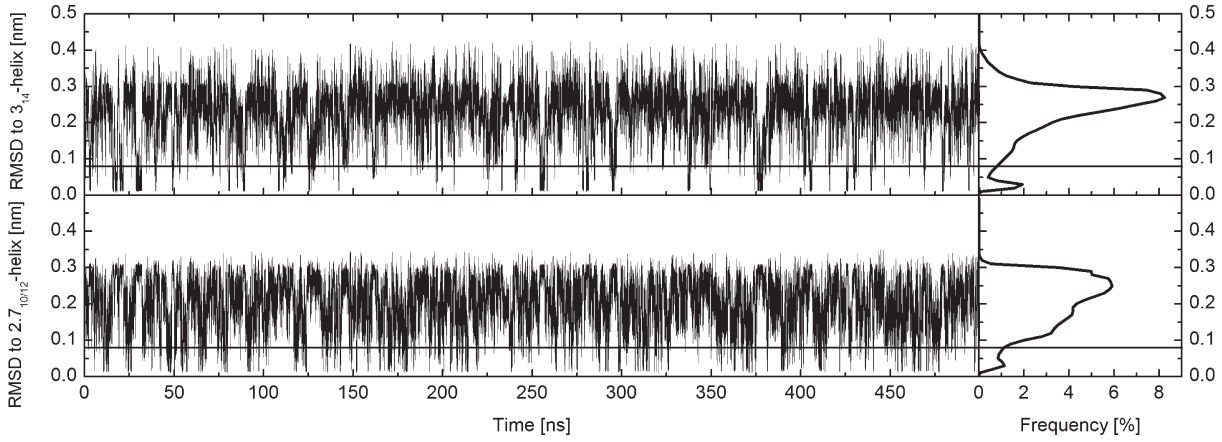

Figure 4. Time evolutions and distributions of the backbone atom-positional rmsd of residues 2−5 of the simulation P_A of peptide **A** with respect to the 3_{14}-helix (upper panels) or the $2.7_{10/12}$-helix (lower panels). The gray lines represent the criterion, an rmsd of 0.08 nm, used to distinguish folded and unfolded conformations.

Table 3. Perturbation Free Enthalpies (kJ mol^{-1}) Associated with Perturbations from the Two Different Helical Reference States of Peptide A to the 16 Peptides with Different Side-Chain Substitutions as Well as the Free Enthalpies between the 3_{14}-Helix and the $2.7_{10/12}$-Helix [a]

	3rd-(β,α), 4th-(β,α)	$\Delta G^{14\text{-helix}}_{pert,ref}$	$\Delta G^{10/12\text{-helix}}_{pert,ref}$	$\Delta G^{14\text{-helix}}_{pert,ref} - \Delta G^{10/12\text{-helix}}_{pert,ref}$ [b]	$\Delta G^{pert}_{14\text{-helix},10/12\text{-helix}}$ [c]
1	(CH_3,CH_3), (CH_3,CH_3)	20.3 ± 0.1	32.2 ± 0.5	−11.9 ± 0.5	−21.3 ± 0.9
2	(CH_3,CH_3),(CH_3,H)	29.5 ± 0.3	36.9 ± 0.2	−7.4 ± 0.3	−16.8 ± 0.8
3	(CH_3,CH_3), (H,CH_3)	28.5 ± 0.1	40.4 ± 0.5	−11.8 ± 0.5	−21.2 ± 0.9
4	(CH_3,CH_3), (H,H)	41.7 ± 0.2	49.3 ± 0.7	−7.6 ± 0.7	−17.0 ± 1.0
5	(CH_3,H), (CH_3,CH_3)	30.3 ± 0.1	35.6 ± 0.4	−5.4 ± 0.4	−14.8 ± 0.9
6	(CH_3,H), (CH_3,H)	39.8 ± 0.1	40.4 ± 0.3	−0.6 ± 0.4	−10.0 ± 0.9
7	(CH_3,H), (H,CH_3)	38.3 ± 0.1	44.7 ± 0.2	−6.4 ± 0.2	−15.8 ± 0.8
8	(CH_3,H), (H,H)	51.6 ± 0.1	53.5 ± 0.3	−1.8 ± 0.3	−11.2 ± 0.8
9	(H,CH_3), (CH_3,CH_3)	29.5 ± 0.1	24.3 ± 1.8	5.2 ± 1.8	−4.2 ± 2.0
10	(H,CH_3), (CH_3,H)	39.5 ± 0.1	30.3 ± 0.6	9.2 ± 0.6	−0.2 ± 0.5
11	(H,CH_3), (H,CH_3)	37.7 ± 0.1	34.5 ± 0.4	3.2 ± 0.4	−6.2 ± 0.9
12	(H,CH_3), (H,H)	51.2 ± 0.2	43.0 ± 0.5	8.1 ± 0.5	−1.3 ± 0.9
13	(H,H), (CH_3,CH_3)	42.6 ± 0.2	38.6 ± 0.4	4.0 ± 0.4	−5.4 ± 0.9
14	(H,H), (CH_3,H)	52.4 ± 0.2	41.8 ± 0.4	10.6 ± 0.5	1.2 ± 0.9
15	(H,H), (H,CH_3)	50.6 ± 0.1	46.5 ± 0.3	4.2 ± 0.3	−5.2 ± 0.8
16	(H,H), (H,H)	64.0 ± 0.2	54.8 ± 0.3	9.2 ± 0.3	−0.2 ± 0.8

[a] The statistical uncertainties were estimated by block averaging.[39] [b] The difference of the first and second numerical columns. If it is negative, the 3_{14}-helical conformation is more stable than the $2.7_{10/12}$-helical one. [c] Folding free enthalpies obtained through eq 4, where the peptide with 3rd-(H,CH_3), 4th-(CH_3,H) is used as H_{pert_0}. See also Figure 2a, with $\Delta G^{pert\_0}_{14\text{-helix},10/12\text{-helix}} = -0.2 \pm 0.5$ kJ mol^{-1}.

are 6.3% for the 3_{14}-helix and 6.0% for the $2.7_{10/12}$-helix. So the free enthalpy difference between the 3_{14}-helix and the $2.7_{10/12}$-helix of H_{pert_0}, i.e., $\Delta G^{pert\_0}_{14\text{-helix},10/12\text{-helix}}$, is −0.2 kJ mol^{-1}. Experiments,[10] quantum-chemical calculations,[11,12] and MD simulations[14] have shown that some β-peptides with an alternating substitution pattern at the α- and β-carbon atoms (β^2-/β^3-peptides) prefer a $2.7_{10/12}$-helical conformation. For peptide **A** which has β^2-Ala and β^3-Ala as the third and fourth residues (Figure 1), the simulation P_A shows that the 3_{14}-helix and the $2.7_{10/12}$-helix are equally populated. A similar β-peptide was simulated before with Leu and Val instead of Ala substituted at the third and fourth residues, respectively, and the fractions of the folded conformation were 2% for the 3_{14}-helix and 16% for the $2.7_{10/12}$-helix in a shorter simulation, i.e., 50 ns, under the same conditions.[14,25] This emphasizes the importance of the side-chain composition to the secondary structure preference of β-peptides.

Free enthalpy differences of perturbing from the two different helical reference states to the 16 real peptides with different side-chain substitution patterns (eq 2) are listed in the first two numerical columns of Table 3. The statistical uncertainties were calculated by block averaging.[39] Because the reference-state simulations were carried out separately for two conformational states, only the relative free enthalpy differences, i.e., $\Delta G^{pert}_{14\text{-helix},10/12\text{-helix}} - \Delta G^{ref}_{14\text{-helix},10/12\text{-helix}}$, could be obtained through $\Delta G^{14\text{-helix}}_{pert,ref} - \Delta G^{10/12\text{-helix}}_{pert,ref}$, shown in the third numerical columns of Table 3. With the simulation of H_{pert_0}, we can, however, get the $\Delta G^{pert}_{14\text{-helix},10/12\text{-helix}}$ values, listed in the last column of Table 3, for all of the perturbed peptides through the second (upper) thermodynamic cycle and eq 4. The statistical uncertainties

of the resulting $\Delta G^{pert}_{14\text{-helix},10/12\text{-helix}}$ values are mostly around 1.0 kJ mol^{-1}. This relatively small value is due to efficient sampling of the helical conformations in the reference-state simulations because of the hydrogen-bond restraining, so the statistical uncertainties of the perturbation free enthalpies are smaller than those of simulations without such restraints.[22] In addition, the long simulation P_A of H_{pert_0} results in a small error bar of $\Delta G^{pert\_0}_{14\text{-helix},10/12\text{-helix}}$.

The resulting free enthalpies, which differ up to 22 kJ mol^{-1}, are mostly negative, which means that the 3_{14}-helical conformation is favored by most of the peptides of set **A**. $\Delta G^{pert}_{14\text{-helix},10/12\text{-helix}}$ may change dramatically upon a change of substitution pattern. The substitution of a methyl group at any X_i position generally favors the 3_{14}-helix. Figure 5 shows $\Delta G^{pert}_{14\text{-helix},10/12\text{-helix}}$ as a function of the number of the CH_3 substitutions at the X_{1-4} positions for peptides of set **A**. The 3_{14}-helix is increasingly favored over the $2.7_{10/12}$-helix as the number of the methyl substitutions increases, by about 5 kJ mol^{-1} per methyl substitution on average. Moreover, methyl substitution at the β-carbon position of the third residue appears to significantly enhance the relative stability of the 3_{14}-helix for peptides of set **A** (Figure 5). Without CH_3 substitution, the 3_{14}-helix and the $2.7_{10/12}$-helix are equally favored by the peptide.

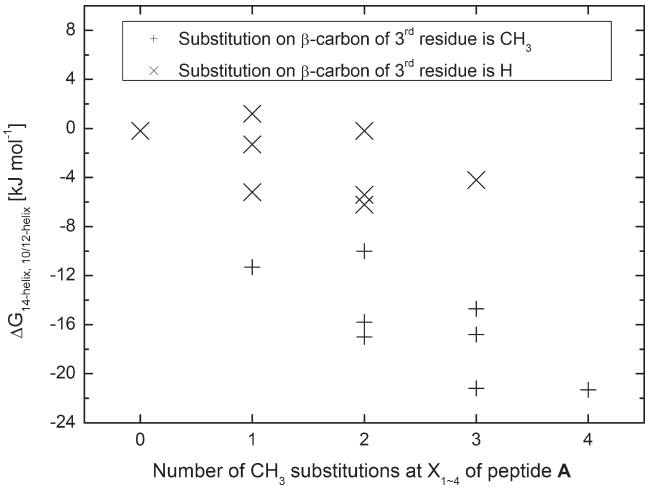

Figure 5. Free enthalpy differences between the 3_{14}-helical and the $2.7_{10/12}$-helical conformations of peptide **A**, $\Delta G^{pert}_{14\text{-helix},10/12\text{-helix}}$, as a function of the number of CH_3 substitutions at the X_{1-4} positions (Figure 1).

It is not straightforward to compare the trends observed in the simulations with those inferred from experimental data,[40] because the latter only provide information on the presence of a particular fold as a function of temperature or solvent composition and do not provide free enthalpy differences between differently folded conformations as reported here. Nevertheless, the patterns of substitutions that favor particular folds are similar.

3.2. Peptide B. The backbone atom-positional rmsds of peptide **B** with respect to the left-handed 3_{14}-helix or the right-handed 2.5_{12}-helix, respectively, of the two reference-state simulations are shown in Figure 6. An rmsd of 0.10 nm (gray horzontal line) was chosen as the criterion to define the different helical conformations $C_{14\text{-helix}}$ and $C_{12\text{-helix}}$. Again, the peptide mainly sampled the folded conformations with unfolding events occurring during the simulations.

The backbone atom-positional rmsds of the simulation P_B of H_{pert_0} with respect to the left-handed 3_{14}-helix and the right-handed 2.5_{12}-helix are shown in Figure 7. The fractions of the folded conformation are 4.0% for the 3_{14}-helix and 1.0% for the 2.5_{12}-helix. These populations are lower than for peptide **A**, but many transitions between the two helical conformations were sampled. The free enthalpy difference between the 3_{14}-helix and the 2.5_{12}-helix of H_{pert_0}, i.e., $\Delta G^{pert\_0}_{14\text{-helix},10/12\text{-helix}}$, is -4.0 kJ mol^{-1}. A similar β-peptide with Val instead of Ala substituted at the fifth residue was simulated before. The fractions of the two folded conformations for that peptide were 8% for the 3_{14}-helix and 5% for the 2.5_{12}-helix in a 100 ns simulation under the same

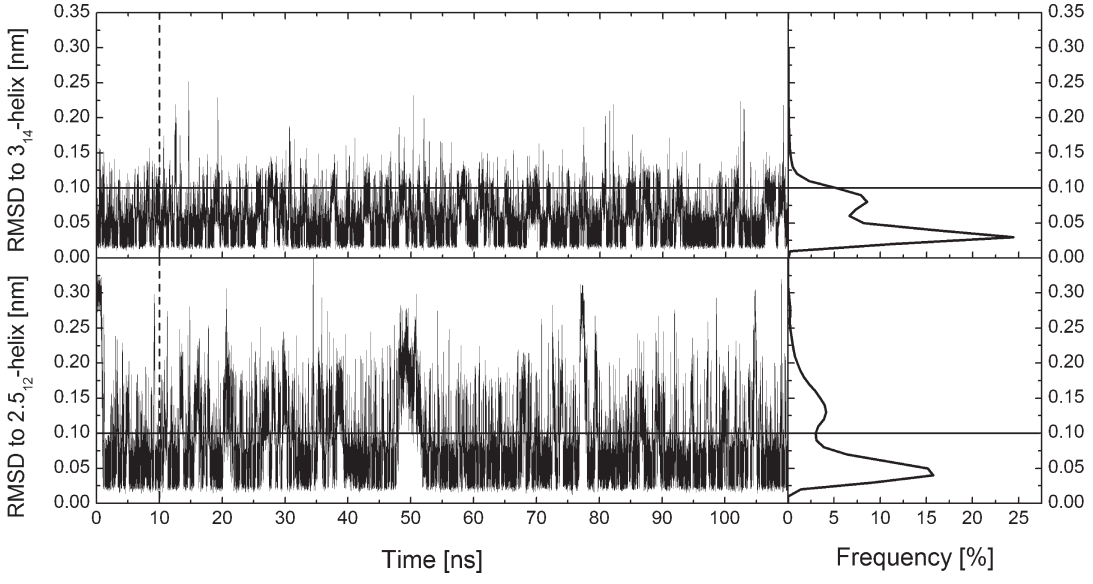

Figure 6. Time evolutions and distributions of the backbone atom-positional rmsd of residues 2−6 of the reference simulations of peptide **B**. Upper panels: Simulation RB_{14} with respect to the 3_{14}-helix. Lower panels: Simulation RB_{12} with respect to the 2.5_{12}-helix. The gray lines represent the criterion, an rmsd of 0.10 nm, used to distinguish folded and unfolded conformations. The first 10 ns were used as equilibration and excluded from calculating distributions.

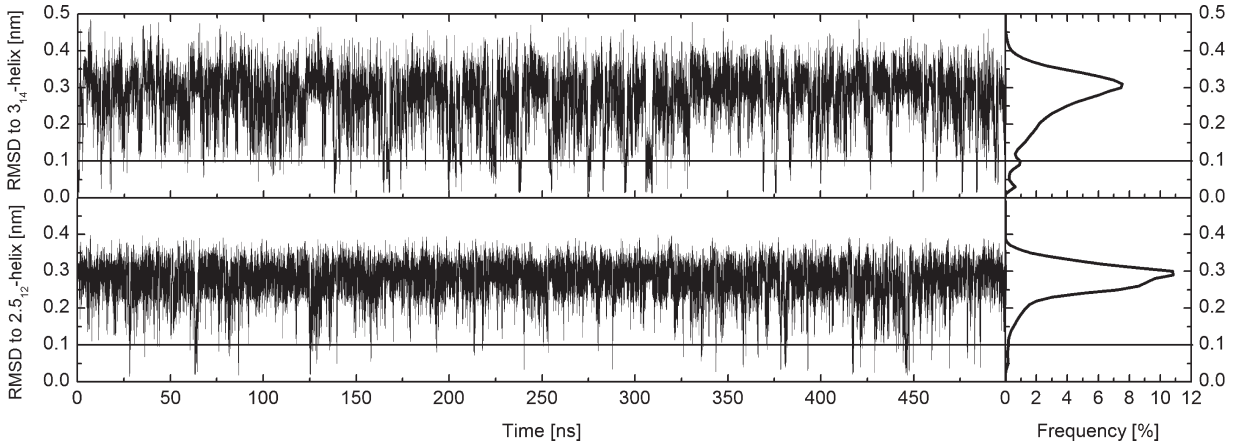

Figure 7. Time evolutions and distributions of the backbone atom-positional rmsd of residues 2−6 of the simulation P_B of peptide **B** with respect to the 3_{14}-helix (upper panels) or the 2.5_{12}-helix (lower panels). The gray lines represent the criterion, an rmsd of 0.10 nm, used to distinguish folded and unfolded conformations.

Table 4. Perturbation Free Enthalpies (kJ mol^{-1}) Associated with Perturbations from the Two Different Helical Reference States of Peptide B to the 16 Peptides with Different Side-Chain Substitutions as Well as the Free Enthalpies between the 3_{14}-Helix and the 2.5_{12}-Helix [a]

	4th-(β,α), 5th-(β,α)	$\Delta G^{14\text{-helix}}_{pert,ref}$	$\Delta G^{12\text{-helix}}_{pert,ref}$	$\Delta G^{14\text{-helix}}_{pert,ref} - \Delta G^{12\text{-helix}}_{pert,ref}$ [b]	$\Delta G^{pert}_{14\text{-helix},12\text{-helix}}$ [c]
1	(CH_3,CH_3), (CH_3,CH_3)	18.3 ± 0.2	29.8 ± 0.5	−11.5 ± 0.5	−10.9 ± 1.3
2	(CH_3,CH_3), (CH_3,H)	26.6 ± 0.9	31.2 ± 0.2	−4.6 ± 0.9	−4.0 ± 0.8
3	(CH_3,CH_3), (H,CH_3)	26.0 ± 0.3	31.5 ± 0.5	−5.5 ± 0.6	−4.9 ± 1.3
4	(CH_3,CH_3), (H,H)	38.4 ± 0.7	42.7 ± 0.8	−4.3 ± 1.0	−3.7 ± 1.6
5	(CH_3,H), (CH_3,CH_3)	28.3 ± 0.2	29.6 ± 0.4	−1.4 ± 0.4	−0.8 ± 1.3
6	(CH_3,H), (CH_3,H)	37.4 ± 0.3	31.3 ± 0.3	6.1 ± 0.4	6.7 ± 1.3
7	(CH_3,H), (H,CH_3)	35.4 ± 0.5	33.1 ± 0.2	2.4 ± 0.6	3.0 ± 1.3
8	(CH_3,H), (H,H)	48.5 ± 0.3	44.0 ± 0.3	4.5 ± 0.4	5.1 ± 1.3
9	(H,CH_3), (CH_3,CH_3)	26.2 ± 0.4	25.7 ± 2.5	0.5 ± 2.5	1.1 ± 2.8
10	(H,CH_3), (CH_3,H)	36.1 ± 0.2	25.6 ± 2.6	10.5 ± 2.6	11.1 ± 2.9
11	(H,CH_3), (H,CH_3)	33.8 ± 0.6	34.1 ± 0.5	−0.3 ± 0.8	0.3 ± 1.4
12	(H,CH_3), (H,H)	47.6 ± 0.3	42.1 ± 2.1	5.6 ± 2.1	6.2 ± 2.4
13	(H,H), (CH_3,CH_3)	39.9 ± 0.2	41.8 ± 0.8	−1.9 ± 0.9	−1.3 ± 1.5
14	(H,H), (CH_3,H)	49.0 ± 0.3	42.5 ± 1.4	6.5 ± 1.4	7.1 ± 1.8
15	(H,H), (H,CH_3)	47.0 ± 0.3	45.6 ± 0.3	1.4 ± 0.4	2.0 ± 1.3
16	(H,H), (H,H)	59.8 ± 0.5	56.0 ± 0.9	3.8 ± 1.0	4.4 ± 1.6

[a] The statistical uncertainties were estimated by block averaging.[39] [b] Difference of the first and second numerical columns. If it is negative, the 3_{14}-helical conformation is more stable than the 2.5_{12}-helical one. [c] Folding free enthalpies obtained through eq 4, where the peptide with 4th-(CH_3,CH_3), 5th-(CH_3,H) is used as H_{pert_0}. See also Figure 2b, with $\Delta G^{pert\_0}_{14\text{-helix},12\text{-helix}} = -4.0 \pm 0.8$ kJ mol^{-1}.

conditions.[25] Apparently, both helical structures are destabilized by changing only one side chain from Val to Ala. The results again show the importance of the side-chain composition to the folding equilibrium of β-peptides.

The perturbation free enthalpies, and $\Delta G^{14\text{-helix}}_{pert,ref} - \Delta G^{12\text{-helix}}_{pert,ref}$, together with $\Delta G^{pert}_{14\text{-helix},12\text{-helix}}$ for all the perturbed peptides of set **B** are shown in Table 4. The free enthalpies differ up to 22 kJ mol^{-1}. The statistical uncertainties of the $\Delta G^{pert}_{14\text{-helix},12\text{-helix}}$ values are larger than those of peptides of set **A**. Generally, they are still smaller than those of unrestrained simulations. As for peptide **A**, the results show that $\Delta G^{pert}_{14\text{-helix},12\text{-helix}}$ may change significantly upon a change of substitution pattern. Having methyl substitutions at both β- and α-carbon positions of the fourth or fifth residue stabilizes the 3_{14}-helix over the 2.5_{12}-helix. Previous studies[11,12,15,24] have shown that β-peptides with substitution exclusively at the β-carbon atom (β^3-peptides) prefer a 3_{14}-helical conformation. In contrast, our one-step perturbation calculations show that peptide **B** with fourth-(CH_3,H), fifth-(CH_3,H), i.e., a β^3-peptide, prefers the 2.5_{12}-helix over the 3_{14}-helix by 6.7 kJ mol^{-1}. This is no cause for concern, because the protonation state of the chain termini has a significant effect on the folding equilibrium of β-peptides due to the so-called "charge dipole stabilization" effect.[25,27] A 201 ns simulation was carried out for a β-peptide having the same sequence as the peptide of the simulation P_B while having NH_3^+ instead of NH_2 at the N-terminus. The backbone atom-positional rmsd is shown in Figure 8. The NH_3^+ terminus shifted the conformational equilibrium strongly toward the 3_{14}-helix. The fraction of the

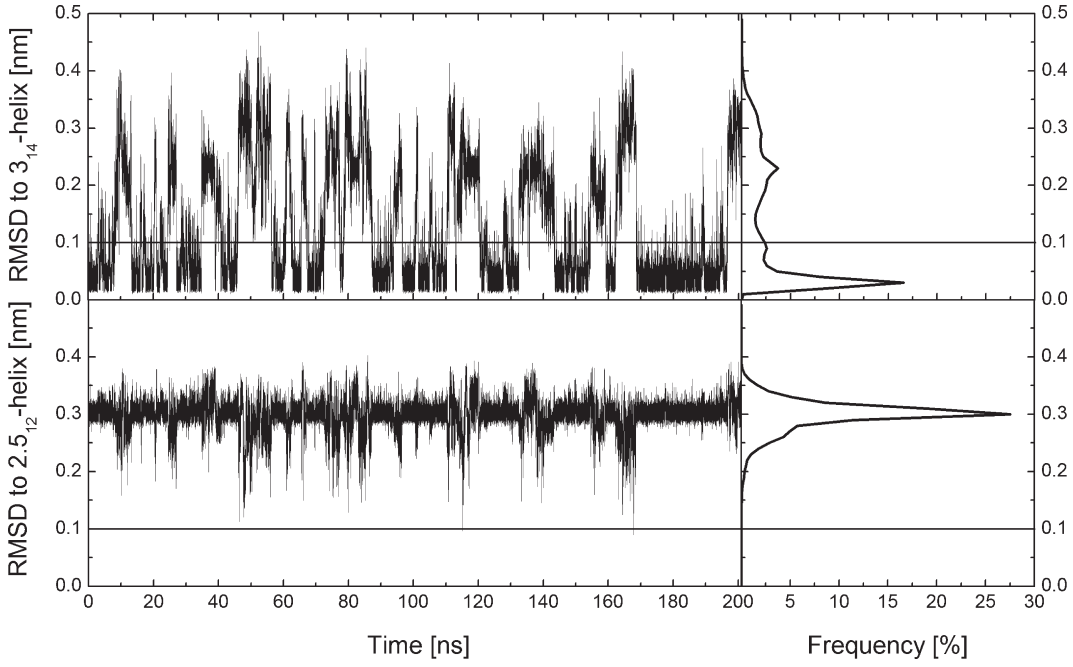

Figure 8. Time evolutions and distributions of the backbone atom-positional rmsd of residues 2−6 of the simulation of peptide H_2^+-β^3-HVal-β^3-HAla-β^3-HLeu-(*S*,*S*)-β^3-HAla(αMe)-β^3-HAla-β^3-HAla-β^3-HLeu-OH with respect to the 3_{14}-helix (upper panels) or the 2.5_{12}-helix (lower panels). The gray lines represent the criterion, an rmsd of 0.10 nm, used to distinguish folded and unfolded conformations.

folded conformation is 52% for the 3_{14}-helix, while almost no 2.5_{12}-helical conformation was sampled. So the use of the NH_2 terminus instead of NH_3^+ for the β^3-substituted peptide **B** may explain its preference for a 2.5_{12}-helical conformation.

4. CONCLUSIONS

Secondary structure preferences of a set of 16 hexa-β-peptides and a set of 16 hepta-β-peptides were investigated by means of one-step perturbation, which method has been shown to be able to predict folding equilibria of β-peptides accurately and efficiently.[21,22] For each peptide, two reference-state simulations and one perturbed-state simulation were carried out to predict the secondary structure preference for the other 15 peptides.

For peptide **A**, the substitution of a methyl group at any X_{1-4} position (Figure 1) stabilizes the 3_{14}-helical conformation. The higher the number of methyl substitutions, the more the left-handed 3_{14}-helix is favored over the right-handed $2.7_{10/12}$-helix. Also, methyl substitution at the β-carbon position of the third residue of peptide **A** is crucial to the relative stability of these two helical conformations. For peptide **B**, having methyl substitutions at both β- and α-carbon positions of the fourth or fifth residue stabilizes the left-handed 3_{14}-helix over the right-handed 2.5_{12}-helix. Because of the presence of a NH_2 terminus instead of NH_3^+ in peptide **B**, the 2.5_{12}-helical conformation is preferred over the 3_{14}-helix by the β^3-substituted peptide. For both peptides, the side-chain substitution patterns have large effects on the relative stabilities of two helical structures, up to 22 kJ mol^{-1} in terms of free enthalpy.

A comparison of the two perturbed-state simulations with previous simulations of two similar peptides which differ in only one or two side chains shows that not only the side-chain substitution pattern but also the composition of the side chains and chain termini affects the secondary structure preference.

One-step perturbation not only reduces the number of required separate simulations by an order of magnitude but also allows prediction of secondary structure preferences for peptides with large free energy differences between two helical conformations, which would be very difficult to obtain by means of long-time simulations. The present study shows that secondary structure preferences of peptides can be efficiently investigated by means of one-step perturbation, which method will facilitate the design of peptides with specific secondary structures and biological activities.

AUTHOR INFORMATION

Corresponding Author

*E-mail: wfvgn@igc.phys.chem.ethz.ch.

ACKNOWLEDGMENT

The authors thank Xiaoye He, Ge Tan, and Bo Wang for their effort in this work. This work was financially supported by the National Center of Competence in Research (NCCR) in Structural Biology and by Grant No. 200020-121913 of the Swiss National Science Foundation, by Grant No. 228076 of the European Research Council (ERC), and by Grant No. IZLCZ2-123884 of the Sino-Swiss Science and Technology Cooperation Program, which are gratefully acknowledged.

REFERENCES

(1) Anfinsen, C. B. *Science* **1973**, *181*, 223–230.
(2) Dobson, C. M. *Nature* **2003**, *426*, 884–890.
(3) MacKerell, A. D. *J. Comput. Chem.* **2004**, *25*, 1584–1604.
(4) van Gunsteren, W. F.; Bakowies, D.; Baron, R.; Chandrasekhar, I.; Christen, M.; Daura, X.; Gee, P.; Geerke, D. P.; Glättli, A.; Hünenberger, P. H.; et al. *Angew. Chem., Int. Ed.* **2006**, *45*, 4064–4092.

(5) van Gunsteren, W. F.; Bürgi, R.; Peter, C.; Daura, X. *Angew. Chem., Int. Ed.* **2001**, *40*, 351–355.
(6) Brooks, C. L. *Acc. Chem. Res.* **2002**, *35*, 447–454.
(7) Daggett, V. *Chem. Rev.* **2006**, *106*, 1898–1916.
(8) Seebach, D.; Matthews, J. L. *Chem. Commun. (Cambridge, U. K.)* **1997**, *21*, 2015–2022.
(9) Martinek, T. A.; Fülöp, F. *Eur. J. Biochem.* **2003**, *270*, 3657–3666.
(10) Seebach, D.; Abele, S.; Gademann, K.; Guichard, G.; Hintermann, T.; Jaun, B.; Matthews, J. L.; Schreiber, J. V. *Helv. Chim. Acta* **1998**, *81*, 932–982.
(11) Wu, Y. D.; Wang, D. P. *J. Am. Chem. Soc.* **1998**, *120*, 13485–13493.
(12) Wu, Y. D.; Wang, D. P. *J. Am. Chem. Soc.* **1999**, *121*, 9352–9362.
(13) Günther, R.; Hofmann, H. J. *Helv. Chim. Acta* **2002**, *85*, 2149–2168.
(14) Daura, X.; Gademann, K.; Jaun, B.; Seebach, D.; van Gunsteren, W. F.; Mark, A. E. *Angew. Chem., Int. Ed.* **1999**, *38*, 236–240.
(15) Glättli, A.; Seebach, D.; van Gunsteren, W. F. *Helv. Chim. Acta* **2004**, *87*, 2487–2506.
(16) Liu, H. Y.; Mark, A. E.; van Gunsteren, W. F. *J. Phys. Chem.* **1996**, *100*, 9485–9494.
(17) Schäfer, H.; van Gunsteren, W. F.; Mark, A. E. *J. Comput. Chem.* **1999**, *20*, 1604–1617.
(18) Oostenbrink, C.; van Gunsteren, W. F. *Proc. Natl. Acad. Sci. U. S. A.* **2005**, *102*, 6750–6754.
(19) Lin, Z. X.; Liu, H. Y.; van Gunsteren, W. F. *J. Comput. Chem.* **2010**, *31*, 2419–2427.
(20) Lin, Z. X.; van Gunsteren, W. F.; Liu, H. Y. *J. Comput. Chem.* **2011**, *32*, 2290–2297.
(21) Lin, Z. X.; Kornfeld, J.; Mächler, M.; van Gunsteren, W. F. *J. Am. Chem. Soc.* **2010**, *132*, 7276–7278.
(22) Lin, Z. X.; van Gunsteren, W. F. *Phys. Chem. Chem. Phys.* **2010**, *12*, 15442–15447.
(23) Lin, Z. X.; Hodel, F. H.; van Gunsteren, W. F. *Helv. Chim. Acta* **2011**, *94*, 597–610.
(24) Seebach, D.; Ciceri, P. E.; Overhand, M.; Jaun, B.; Rigo, D.; Oberer, L.; Hommel, U.; Amstutz, R.; Widmer, H. *Helv. Chim. Acta* **1996**, *79*, 2043–2066.
(25) Lin, Z. X.; Schmid, N.; van Gunsteren, W. F. *Mol. Phys.* **2011**, *109*, 493–506.
(26) Zwanzig, R. W. *J. Chem. Phys.* **1954**, *22*, 1420–1426.
(27) Gee, P. J.; van Gunsteren, W. F. *Proteins: Struct., Funct., Bioinf.* **2006**, *63*, 136–143.
(28) van Gunsteren, W. F.; Billeter, S. R.; Eising, A. A.; Hünenberger, P. H.; Krüger, P.; Mark, A. E.; Scott, W. R. P.; Tironi, I. G. *Biomolecular Simulation: The GROMOS96 Manual and User Guide*; Vdf Hochschulverlag AG an der ETH Zürich: Zürich, Switzerland, 1996.
(29) Christen, M.; Hünenberger, P. H.; Bakowies, D.; Baron, R.; Bürgi, R.; Geerke, D. P.; Heinz, T. N.; Kastenholz, M. A.; Kräutler, V.; Oostenbrink, C.; et al. *J. Comput. Chem.* **2005**, *26*, 1719–1751.
(30) Schuler, L. D.; Daura, X.; van Gunsteren, W. F. *J. Comput. Chem.* **2001**, *22*, 1205–1218.
(31) Daura, X.; Antes, I.; van Gunsteren, W. F.; Thiel, W.; Mark, A. E. *Proteins: Struct., Funct., Genet.* **1999**, *36*, 542–555.
(32) Daura, X.; van Gunsteren, W. F.; Mark, A. E. *Proteins: Struct., Funct., Genet.* **1999**, *34*, 269–280.
(33) Berendsen, H. J. C.; Postma, J. P. M.; van Gunsteren, W. F.; DiNola, A.; Haak, J. R. *J. Chem. Phys.* **1984**, *81*, 3684–3690.
(34) Ryckaert, J. P.; Ciccotti, G.; Berendsen, H. J. C. *J. Comput. Phys.* **1977**, *23*, 327–341.
(35) Tironi, I. G.; Sperb, R.; Smith, P. E.; van Gunsteren, W. F. *J. Chem. Phys.* **1995**, *102*, 5451–5459.
(36) Walser, R.; Mark, A. E.; van Gunsteren, W. F.; Lauterbach, M.; Wipff, G. *J. Chem. Phys.* **2000**, *112*, 10450–10459.
(37) Beutler, T. C.; Mark, A. E.; van Schaik, R. C.; Gerber, P. R.; van Gunsteren, W. F. *Chem. Phys. Lett.* **1994**, *222*, 529–539.
(38) Daura, X.; Jaun, B.; Seebach, D.; van Gunsteren, W. F.; Mark, A. E. *J. Mol. Biol.* **1998**, *280*, 925–932.
(39) Allen, M. P.; Tildesley, D. J. *Computer Simulation of Liquids*; Oxford University Press: New York, 1987.
(40) Seebach, D.; Beck, A. K.; Bierbaum, D. J. *Chem. Biodiversity* **2004**, *1*, 1111–1239.